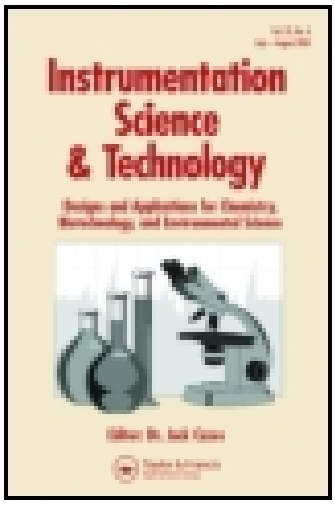

Instrumentation Science & Technology
Publication details, including instructions for authors and subscription information:
http://www.tandfonline.com/loi/list20

Characterization of the Corrosion of Iron Using a Smartphone Camera

D. Igoe[a] & A. V. Parisi[a]
[a] Faculty of Health, Engineering and Sciences, University of Southern Queensland, Toowoomba, Australia
Accepted author version posted online: 21 Aug 2015.

To cite this article: D. Igoe & A. V. Parisi (2015): Characterization of the Corrosion of Iron Using a Smartphone Camera, Instrumentation Science & Technology, DOI: 10.1080/10739149.2015.1082484

To link to this article: http://dx.doi.org/10.1080/10739149.2015.1082484

Characterization of the Corrosion of Iron Using a Smartphone Camera

D. Igoe[1], A. V. Parisi[1]

[1]Faculty of Health, Engineering and Sciences, University of Southern Queensland, Toowoomba, Australia

To whom correspondence is to be addressed E-mail: damienpaul@gmail.com

Abstract

Smartphone technology provides bountiful opportunities for greater participation in scientific and technological research. Digital camera image sensors have been used for the detection, measurement, and monitoring of corrosion; this work extends that capability to the smartphone. It has been observed that as the corrosion increased in clean iron, red responses decreased proportionally. Green and blue responses quantifiably decreased faster, matching the observed overall reddening as the corrosion increased. Potential noise sources due to the variable texture of the corroded samples had a negligible effect on the results. The effectiveness of this method for the characterization of a smartphone image sensor response to the degree of iron corrosion was reflected in congruent validation tests and errors less than 5%. These results demonstrate that the smartphone may be employed as a low cost and efficient means for the evaluation of surface corrosion.

KEYWORDS: Smartphone, corrosion, image sensor

INTRODUCTION

Smartphone technology is ubiquitous and the inherent processing power, programmability, and sensor arrays are generally underutilized. There has been considerable work in the application of smartphone technology for scientific and technological applications; examples include solar measurements [1], bacteriological imaging [2], and seismographs [3]. Smartphone use for scientific and technological investigations provides an opportunity for wider participation in these endeavours [1]. This research extends the use of the smartphone image sensor to determine the concentration of iron that has corroded.

Corrosion, particularly of iron, is of great mutual concern of those in industry and construction, home-owners, and those who love their cars. Corrosion is a natural process that can be accelerated due to the presence of aerosol pollution [4-6]. Corrosion is not only aesthetically displeasing to look at, it is of major concern to those who rely on the stability and strength of iron and iron based alloys, such as steel [5-6]. The effects of corrosion are costly, with an estimated cost to the United States economy in 1999 and 2001 of $276 billion dollars per year, or just over 3% of the gross national product [4].

There is a necessity to monitor the integrity of iron, particularly when exposed to areas of high pollution, airborne salinity, and humidity. Practicalities demand that any monitoring and detection of corrosion to be nondestructive [5]. Qi and Gelling [5] summarized the main sensors used to detect corrosion as being one or a combination of electromagnetic, electrochemical, optical fluorescent, and optical fiber mechanisms, all based on the chemical, galvanic, and optical properties. In pipes, fiber optic systems have proven to be

invaluable in detecting corrosion [7-8]. For concrete reinforcement, the use of impedance capacitive sensors has been found to be effective in alerting people to corrosion that is not visible [9].

Digital image processing has also been used in the detection and monitoring of surficial corrosion. Laboratory tests successfully demonstrated that the corrosion processes may be monitored using digital speckle pattern interferometry [10]. Digital cameras have been used for the detection of corrosion; particularly; the onset of the process. The color due to the degree of corrosion was used as a basis of a Support Vector Machine [11]. Perlin Noise has been used to simulate oxide corrosion textures to provide a means for visual estimation of the amount of corrosion present in a sample quickly and accurately for onsite inspections [6].

The image sensor used in a smartphone is based on complementary metal oxide semiconductor (CMOS) technology [12]. Typically, images are saved in smartphones in jpeg format, with the intensity of each of the red, green, and blue responses in each pixel scaled as integers from 0 to 255 [13]. Smartphones are not designed to provide full spectral data, but the color responses may be calibrated to quantify the magnitude and change in incident light [1]. However, previous work has found that each smartphone image sensor has differences in their response, due to various manufacturing methodologies [1], so this study provides a method to characterize corrosion concentration. Smartphone image sensors have been shown to have a negligible dark noise response [13].

A key factor when developing corrosion monitoring systems is that any system needs to be easy to use and require minimal computational processing power to develop a model for corrosion formation [4, 6]. The development of this method used a smartphone and freely available image processing tools, as demonstrated in previous work [1-3]. This study demonstrates the characterization of corrosion using an inexpensive smartphone image sensor.

METHOD AND MATERIALS

The smartphone used was an LG L3 (LG Electronics, Seoul, South Korea). The smartphone was Wi-Fi and Bluetooth enabled, allowing images to be sent directly to a laptop. Image analysis, including developing histograms for grey (Y), red (R), green (G), and blue (B) responses (scaled to 255) [13] and statistical data (mean and standard error) of each image were determined using a freeware Java based image processing program called *ImageJ*.

Clean square tiles (20 mm x 20 mm) were cut from an iron sheet. Corroded iron square tiles (20 mm x 20 mm) were prepared by immersing pristine iron samples in saline water. Other tiles were maintained in a pristine state. All samples were kept clear of other contaminants, such as dirt and dust.

Each image was taken 1 m directly above an arrangement of 5 x 5 squares, with different numbers of corroded and uncorroded tiles used firstly in geometric patterns for calibration and then randomly scattered with different amounts of corroded tiles for

model validation. Each image contained approximately 63,000 pixels. For consistency in the characterization, the calibration arrangements and the samples for the validation were illuminated by a D65 daylight lamp placed 2 m above the samples.

The images were sent from the smartphone to a laptop and saved. These images were individually opened in *ImageJ*. The average R, G, and B values were obtained by the following menu commands: *Plugins* → *Analyze* → *RGB Measure*. The Grey response (Y), representing the overall reflected light intensity from each sample was calculated by [13]

$$Y = 0.3R + 0.59G + 0.11B \quad [1]$$

where R, G, and B represent the red, green and blue pixel values from the smartphone image sensor.

Initially for calibration, 5 x 5 arrangements were made of pristine iron tiles and separately corroded iron tiles. A geometric pattern of corrosion from the center and from the edges were processed. The tiles were placed on a nonreflective neutral grey card. The arrangements of the tiles are shown in Figure 1.

The calibration models were validated by further arrangements with a scattered distribution of corroded iron tiles within the 5 x 5 grid. Ten pictures were taken for each arrangement and the standard error calculated for each. The grey, red, green, and blue responses using the calibration equations were compared with the values derived from the validation images. Further validation was performed using three pieces of corroded iron

found in the surrounding area. These samples were characterized using the same method as for calibration and validation measurements.

RESULTS

Several distinct and quantifiable patterns emerged from the image analysis. The histograms revealed that the presence of increasing corrosion caused a peak with a center digital value of approximately 73 to increase. At the same time, a decreasing and merging trend was visible in a double peak at digital values of approximately 151 and 170 (Figure 2). Although the position of the lower intensity peak was different, the same trend was present for all red, green, and blue channels.

CALIBRATION

The grey response had a negative relationship with the percentage corrosion in each sample, starting from the approximate value for the sample with no corrosion $(C_{0\%})$. This relationship has a coefficient of determination of 0.99. The relationship between grey response (Y) to percentage corrosion $(C_{0\%})$ is in equation 2.

$$Y = C_{0\%} - 1.06C_{\%} \quad [2]$$

The red response (R) exhibited a 1:1 decline with increasing corrosion, whereas the decrease in the green (G) and blue (B) responses were steeper:

$$R = C_{0\%} - C_{\%} \quad [3]$$

$$G = C_{0\%} - 1.12C_{\%} \quad [4]$$

$$B = C_{0\%} - 1.15C_{\%} \quad [5]$$

Validation

Smartphone images of scattered corrosion and the corrosion on the three random samples were used to validate the calibration relationships and demonstrated a coherent match to modelled values using equations (1), (2), (3), (4), and (5). A comparison between the observed Y, R, G, and B values from corroded samples and the equivalent modelled values from the calibration tests are shown in Table 1.

DISCUSSION

Overall, as the corrosion in each sample increased, the images' grey and red response decreases (darkens) at the same rate, and the green and blue responses darken faster, with blue darkening the fastest. Figure 3 demonstrates that as the corrosion concentration increased, the grey value darkened, increasing the count of pixels possessing the same grey value as the 100 % corroded sample while not expanding the peak width. At the same time, the higher value bimodal peak collapsed into a smaller single broad peak.

Despite the random variations observed in the texture of the corroded tiles [6], the grey response with increasing concentration and the position of the peak remained consistent. This is especially significant as different tiles were used in each trial, demonstrating that the variability of texture did not result in excess noise in each image. Further, the positioning of the tiles, from a patterned configuration in the calibration tests to random placements for validation did not have any significant effect on the grey response trend.

Red, green, and blue responses also decreased, but at different rates. Equations (3), (4), and (5) represent mathematical models of corrosion growth [4] as detected by a smartphone camera. On visual inspection, the iron oxide is dark red, implying that there is a minimal deviation in the red while there is a steeper decrease in the green and blue responses. The red response darkens at the rate that the percentage of corrosion increases, demonstrating that the red response is an indicator of the degree of corrosion, provided that the initial pristine amount is known (in equation 2). This approach is similar to the Support Vector Machine method, but using a less complicated, resource consuming approach [4, 11]. When compared to the red response, the green and blue responses demonstrate a linear relationship with coefficients of determination of 0.99 for both.

When the green and blue responses are compared to the red, the relationships are very similar to their response to increasing corrosion as shown by

$$G = 1.13R - 21 \qquad [6]$$

$$B = 1.18R - 29 \qquad [7]$$

However, when the green and blue channel responses are normalized to red responses (G' and B' respectively) and compared to the proportion of corrosion, the relationship is a broad negative parabola (Figure 4). The coefficients of the parabola are less than 10^{-4}. These relationships are significantly weaker than their calibrated values, with coefficients of determination for G' and B' of 0.88 and 0.93, respectively:

$$G' = -2\times10^{-5} C_{\%}{}^{2} + 0.0003 C_{\%} + 1 \qquad [8]$$

$$B' = -2\times10^{-5} C_{\%}{}^{2} + 0.0002 C_{\%} + 1 \qquad [9]$$

The decrease in Figure 4 is consistent with the green and blue response calibration. The broad parabolic nature of the relationship is likely to be an artifact of the corrosion texture, as the divergence from the lines increases with increasing corrosion. The normalization of the green and blue responses reveal that there was a reduction of up to 18% and 25% in their intensities.

The scattering of the corroded pieces for the validation measurements introduced errors of 1.7%, 1.1%, and 2.4% with the calibrated models for the red, green and blue responses, respectively. There were no discernible patterns in errors with increasing corrosion. However, the red response errors were generally positive while green and blue errors were generally negative (Figure 5). This suggests that the smartphone image sensor marginally compensated for the red response at the expense of the green and blue responses. However, these errors are small and were within 5% of modelled values.

CONCLUSIONS

Varying amounts of red iron corrosion were characterized using a smartphone sensor, with images analyzed by a simple Java processing program. Models for red, green, and blue responses to corrosion were quantified. The red response exhibited a very strong inverse 1:1 relationship with the percentage of corrosion, with the green and blue responses having a quantifiably steeper regression. These results demonstrate that the smartphone image sensor quantified the reddening and dimming of the iron with increasing corrosion. Errors in all three color responses were within 5%, similar to what was found using the Perlin noise based models [6]. These measurements indicated that

the variable texture of the corroded surface did not cause significant noise in the image sensor, demonstrating that the smartphone is a low cost and efficient means of evaluating surface corrosion.

ACKNOWLEDGMENT

We wish to acknowledge the Faculty of Health, Engineering and Sciences workshop for the preparation of the iron and corroded materials used in this study.

REFERENCES

1. Igoe, D.; Parisi, A; Carter, B., Evaluating UVA aerosol optical depth using a smartphone camera, Photochem. Photobiol., 2013, 89 (5), 1244-1248.

2. Breslauer, D.; Maamari, R.; Switz, N.; Lam, W.; Fletcher, D., Mobile phone based clinical microscopy for global health applications, PLoS ONE, 2009, 4 (7), 1-6.

3. Feng, M.; Fukuda, Y.; Mizuta, M.; Ozer, E. Citizen Sensors for SHM: Use of accelerometer data from smartphones, Sensors, 2015, 15 (2), 2980-2998.

4. Choudhary, P.; Anand, R. Determination of rate of degradation of iron plates due to rust due to rust using image processing, Int. J. Eng. Res. 2015, 4 (2) 76-84

5. Qi, X.; Gelling, V. A review of different sensors applied to corrosion detection and monitoring, Rec. Patents in Corr. Sci. 2011, 1 (1), 1-7.

6. Acosta, M.; Diaz, J.; Castro, N. An innovative image-processing model for rust detection using Perlin Noise to simulate oxide textures, Corr. Sci. 2014, 88, 141-151.

7. Rajeev, P.; Kodikara, J.; Chiu, W.; Kuen, T. Distributed optical fibre sensors and their application in pipeline monitoring Key Eng. Mat. 2013, 558, 424-434.

8. Lee, J.; Yun, C.; Yoon, D. A structural corrosion monitoring sensor based on a pair of prestrained fiber Bragg gratings, Meas. Sci. Tech. 2010, 21, 017002.

9. Rahman, S.; Ismail, M.; Noor, N.; Bakhtiav, H. Embedded capacitor sensor for monitoring corrosion of reinforcement in concrete, J. Eng. Sci. Tech. 2012, 7 (2), 209-218.

10. Andres-Arroyo, A.; Andres, N.; Palero, V.; Arroyo, M.; Angurel, L. Possibilities and limitations of digital speckle pattern interferometry in the analysis of corrosion processes in metallic materials, Meas. Sci. Tech. 2013, 24, 075204.

11. Sharma, V.; Thind, T. Techniques for detection of rusting of metals using image processing: A survey, Int. J. Emerg. Sci. Eng, 2013, 1 (4), 60-62.

12. Hayes, T. Next-generation cell phone camera, Opt. Phot. 2012, 23, 17-21.

13. Igoe, D.; Parisi, A.V.; Carter, B. A method for determining the dark response for scientific imaging with smartphones, Inst. Sci. Tech. 2014, 42 (5), 586-592.

14. Jost, T.; Ouerhani, N.; von Wartbug, R.; Muri, R.; Hugli, H. Assessing the contribution of color in visual attention, Comp. Vis. Im. Und. 2005, 100 (1-2), 107-123.

Table 1 Comparison of red, green and blue responses to corroded materials with calibration equations.

	Measured Response			Modelled Response		
Corrosion, %	Red	Green	Blue	Red	Green	Blue
10	168	162	162	165	165	164
50	123	117	116	124	122	119
100	83	70	68	73	61	58

Figure 1. Arrangement of pristine and corroded iron tiles. Corroded tiles are shaded.

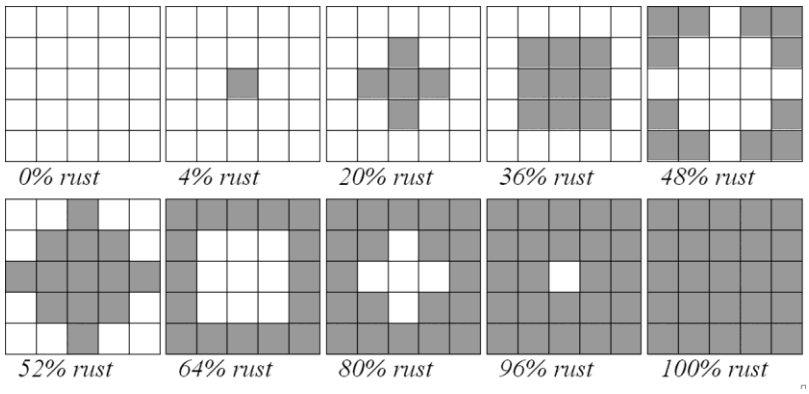

Figure 2. Combined histogram for the grey response of 20% (grey dashed line), 48% (black dashed line) and 80% (black line) corrosion.

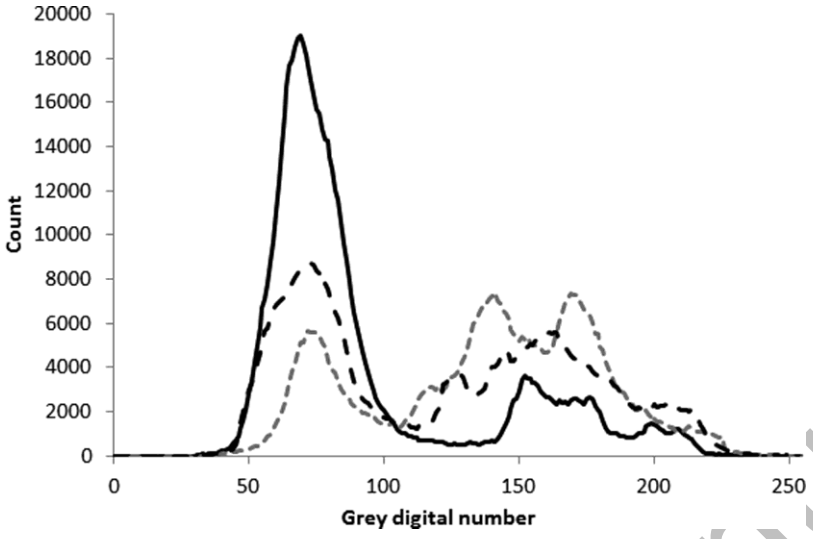

Figure 3. Relative darkening of the grey response with increasing corrosion. As corrosion increased, the grey response decreases to the lower peak (A), resulting in a consistent increase without widening (B), and causes a subsequent decrease of the upper values (C).

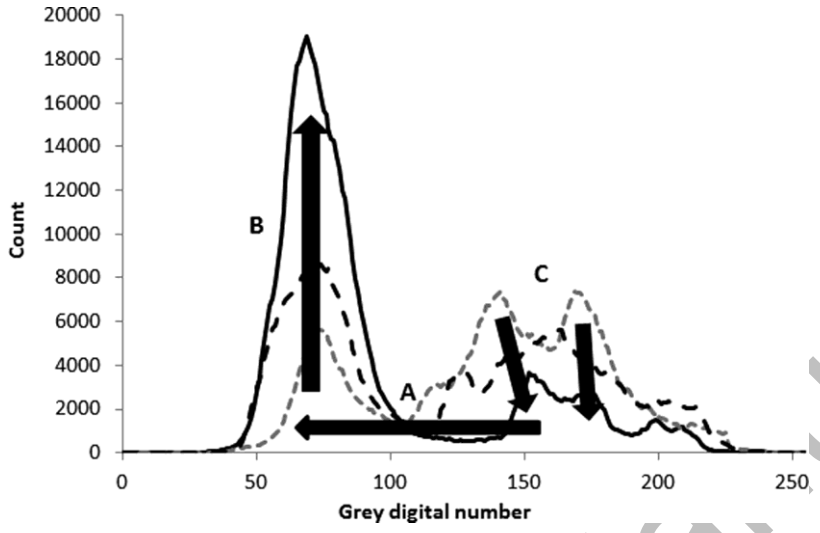

Figure 4. Green (diamonds and full line) and blue (squares and dashed line) responses normalized to red response plotted against the degree of corrosion.

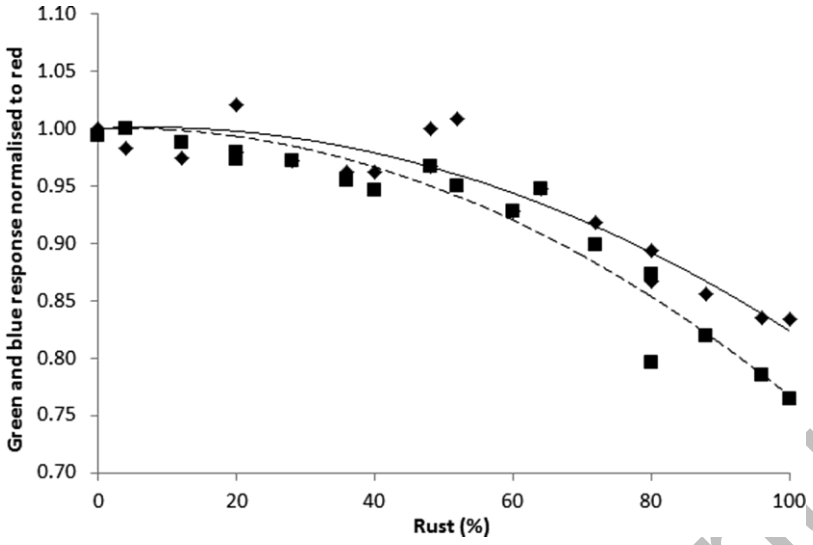

Figure 5. Error between the measured and modelled red (diamonds), green (squares), and blue (triangles) responses with respect to the percentage of corrosion.